

EFFECT OF STRUCTURAL RELAXATION ON THE DEFORMATION BEHAVIOR OF A $Zr_{64.13}Cu_{15.75}Ni_{10.12}Al_{10}$ BULK METALLIC GLASS UNDER NANOINDENTATION

JIANSHENG GU*

*National Microgravity Laboratory, Institute of Mechanics, Chinese Academy of Sciences, Beijing 100190, China

BINGCHEN WEI^{†§}, TAIHUA ZHANG[‡], YIHUI FENG[‡], YANPING HU[†] and ZHIWEI SUN[†]

[†]National Microgravity Laboratory, Institute of Mechanics, Chinese Academy of Sciences, Beijing 100190, China

[‡]State Key Laboratory of Nonlinear Mechanics(LNM), Institute of Mechanics, Chinese Academy of Sciences, Beijing 100190, China
[§]weibc@imech.ac.cn

Received 8 October 2008

Structural relaxation by isothermal annealing below the glass transition temperature is conducted on a $Zr_{64.13}Cu_{15.75}Ni_{10.12}Al_{10}$ bulk metallic glass. The effect of structural relaxation on thermal and mechanical properties was investigated by differential scanning calorimetry and instrumented nanoindentation. The recovery of the enthalpy in the DSC curves indicates that thermally unstable defects were annihilated through structural relaxation. During nanoindentation, the structural relaxation did not have a significant influence on the serrated plastic flow behavior. However, Structural relaxation shows an obvious effect in increasing both the hardness and elastic modulus, which is attributed to the annihilation of thermally unstable defects that resulted from the relaxation.

Keywords: Bulk metallic glass; structural relaxation; defects; shear bands.

1. Introduction

Bulk metallic glasses (BMGs) have attractive mechanical properties such as outstanding strength, elastic strain, and elastic energy storage, but their low ductility at room temperature severely hindered them as structural materials[1]. Consequently, much attention has currently been paid to understanding the deformation mechanism and finding ways to improve the plasticity of BMGs [2-8].

It is well known that material behaviors, especially mechanical properties, are controlled by defects. The concept of defects in metallic glasses appears in the application of the free-volume theory to the mechanism of plastic flow [9, 10]. A defect is defined as a site at which the free volume exceeds a critical value, which is on the order of an atomic volume. Metallic glass can lie in different energy levels depending on the number of structural defects frozen in the sample during quenching. When annealed at a temperature that is high enough to allow some atomic motion but still sufficiently

low to avoid rapid crystallization, they relax to a series of states with continuously lower free energy. This phenomenon is known as structural relaxation, a process which is generally believed to be mainly characterized by annihilation of excess free volume or structural defects [11]. Early work on metallic glass films and BMGs has shown that most metallic glasses exhibit a marked loss in ductility upon annealing below the glass transition temperature [12-14]. Furthermore, to examine the effect of excess free volume and relaxation state on the plastic deformation behavior of metallic glasses is of interest, as this could provide insight on the correlation between defects (or free volume) with the plastic deformation mechanics in metallic glasses. Recently, some work has been done to study the plastic flow behavior of metallic glasses with different free volume concentration, utilized by controlling the quenching rates or by annealing below glass transition temperature (T_g). The serrated flow behavior is found to be sensitive to the free volume concentration, i.e. more free volume promotes conspicuous serration with large pop-in size [15, 16]. In contrast, there are also experimental results exhibiting that the change of free volume does not exert a distinct influence on plastic flow behavior [17, 18]. Thus, it is evident that more work should be done for further understanding the effect of free volume (or atomic scaled defects) on the plastic flow behavior in BMGs. In this work, $Zr_{64.13}Cu_{15.75}Ni_{10.12}Al_{10}$ BMG [3], one of the most ductile BMGs up to now, is used to obtain different relaxation states by annealing at sub- T_g for various durations. The free volume effect on mechanical properties and serrated flow during plastic deformation is studied by nanoindentation.

2. Experimental Procedures

The alloy used in the present study is the $Zr_{64.13}Cu_{15.75}Ni_{10.12}Al_{10}$ BMG that possesses excellent plasticity and a wide supercooled liquid region [3]. Cylindrical rods of $Zr_{64.13}Cu_{15.75}Ni_{10.12}Al_{10}$ BMG in 3mm diameter were prepared by arc-melting a mixture of elements with purities higher than 99.9% followed by suction-casting. The isothermal annealing treatment was performed at 590K, which is lower than T_g (645K). The as-cast and the relaxed specimens were determined to be amorphous based on X-ray diffraction. Differential-scanning calorimetry (DSC, NETZSCH DSC-404C) was used to characterize the thermal properties of the BMGs.

The specimens for nanoindentation measurements were mechanically polished to a mirror finish and tested in an MTS Nano Indenter XP fitted with a Berkovich indenter. Indentations were all performed to a depth limit of 1000nm with a load holding segment of 10s in at the maximum depth. The loading processes of indentation were carried out under a load control mode at loading rates of 0.075mN/s, 0.2mN/s, 0.5mN/s and 1mN/s, respectively. The thermal drift of the instrument was maintained below 0.05nm/s. The deformation morphology around the indents after nanoindentation was checked by scanning electron microscopy (SEM) and atomic force microscopy (AFM).

3. Results and Discussion

DSC thermograms of the as-cast and relaxed samples annealed for 1, 6 and 24 h,

respectively, are shown in Fig. 1. All samples exhibit very similar values of T_g , the onset temperature of crystallization (T_x), and the width of supercooled liquid region (ΔT_x), as list in Table 1. It can be also seen in Fig. 1 that an endothermic overshoot in the vicinity of glass transition, which stands for the enthalpy recovery during heating, can be clearly observed in the annealed samples. The enthalpy recovery peak was found to increase in magnitude with annealing time as indicated in the inset of figure 1. The amount of the recovered enthalpy ΔH is determined from the area between the curve of the relaxed sample and the as-cast sample. The recovered enthalpy supposed to be proportional to the change in the average free volume during structural relaxation [19,20]

$$v_f / v_m = C\Delta H \quad (1)$$

Where C is a constant, v_m is the atomic volume. Only the local free volume of an atom becomes larger than some critical value, v^* , can the atom escape from its nearest neighbor cage and contribute to the plastic deformation flow behavior, i.e. it becomes part of a defect [10]. The defect concentration can be calculated from the statistical distribution of the free volume among all the atoms and expressed as

$$c_D = \exp(-v_f / \gamma v^*) \quad (2)$$

Where γ is a geometrical factor on the order of unity. From eqs. (1) and (2), it can be recognized that thermally unstable defects which are annihilated during sub- T_g annealing is proportional to the enthalpy recovery variation ΔH . Accordingly, the as-cast sample has a maximum value of defect concentration frozen from quenching, and the defect concentration decrease continuously with increasing annealing time.

Table 1. Thermal and mechanical properties of the as-cast and relaxed $Zr_{64.13}Cu_{15.75}Ni_{10.12}Al_{10}$ BMGs.

BMGs	T_g (K)	ΔT_x (K)	ΔH (J/g)	H (GPa)	E (GPa)
As-cast	647	99	--	5.95±0.10	94.20±1.85
1h	650	95	6.60	6.18±0.07	99.32±2.35
6h	650	94	7.45	6.19±0.02	101.86±0.63
24h	650	93	8.37	6.21±0.07	102.40±0.76

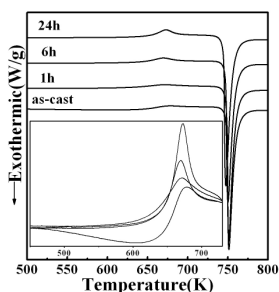


Fig. 1. The DSC curves of as-cast sample and pre-annealed samples for different times of $Zr_{64.13}Cu_{15.75}Ni_{10.12}Al_{10}$ BMG. Insets are enlarged DSC curves around the glass transition region.

To examine the effect of thermally unstable defects on mechanical properties and plastic deformation behavior of the $Zr_{64.13}Cu_{15.75}Ni_{10.12}Al_{10}$ BMGs, instrumental nanoindentation measurements were carried out on the as-cast and relaxed samples. The hardness and elastic modulus obtained from the $P-h$ curves of nanoindentations at loading rate 0.02mN/s are listed in Table 1. These properties show a close relationship with thermally unstable defects. The as-cast sample, in which the largest amount of unstable defects are preserved, has the smallest hardness of 5.95GPa and modulus of 94.20GPa, respectively. The hardness and modulus increase with increasing annealing time. For the 24-hour annealed sample, in which the thermally unstable defects have been annihilated almost thoroughly, has maximum hardness and modulus 6.21GPa and 102.40GPa respectively.

The serrated flow phenomenon can clearly be observed during the loading process of nanoindentation for all alloys, and they become less obvious with increasing loading rates. Typical load-depth ($P-h$) curves of the as-cast and relaxed samples (annealed for 1, 6 and 24 hours, respectively) results at loading rate of 0.2mN/s are shown in Fig. 2(a).. To clearly characterize the serration feature in the load-depth curves, the load plotted as a function of the depth at various loading rates was simulated as an exponential function

$$P_{fit} = Kh^m \quad (3)$$

where K and m are constant. The function

$$\Delta P = P_{exp} - P_{fit} \quad (4)$$

describes the range of serrations, where P_{exp} is the experimental value. Fig. 2(b) shows $\Delta P-h$ curves for the four samples during nanoindentation at loading rate of 0.2mN/s. These curves highlight the serration behavior observed in the load-depth curves. It can be seen that the as-cast and relaxed samples exhibit quite similar serrated flow features, without obvious change of number and size of pop-ins. Serrations displayed in the $P-h$ curves during nanoindentation are related to the formation and operation of individual shear bands [21-23]. The obvious serrations in the $P-h$ curves of the samples at all relaxation states (Fig. 2) indicate that the plastic deformation of the as-cast and relaxed samples is highly inhomogeneous. These prove that the serrated flow feature in present $Zr_{64.13}Cu_{15.75}Ni_{10.12}Al_{10}$ BMG is insensitive to defect concentration. In other words, the isothermal structural relaxation for up to 24 h at about 55 K lower than T_g , does not significantly affect the serrated flow behavior of this alloy.

To further understand the deformation dependence on thermally unstable defects, the surface morphologies of indents during nanoindentation were all examined by SEM and AFM. Typical AFM topography of the the as-cast and annealed alloys are shown in Fig. 3. There are obvious pile-ups containing shear bands around the indents in both as-cast and annealed 24-hour samples. The number of shear bands and the height of the pile-up around are similar in both alloys, though the relaxed alloy possesses a much lower concentration of thermal unstable defects than that of the as-cast alloy.

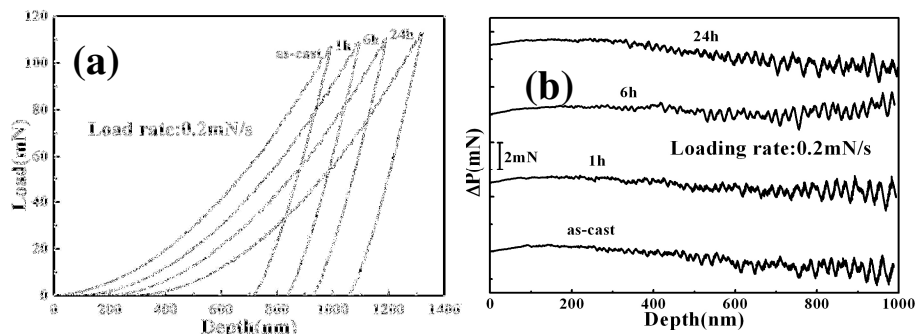


Fig. 2. Typical load-depth (P - h) curves (a) and ΔP - h curves (b) of the as-cast and relaxed samples during nanoindentation at loading rates of 0.2mN/s.

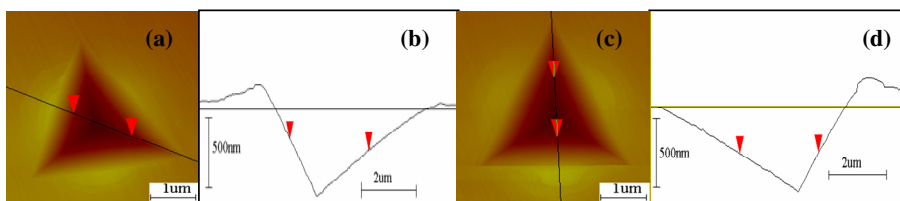


Fig. 3. AFM images and corresponding height profiles of the indents at loading rate 0.2mN/s after nanoindentation: (a) (b) as-cast sample, (c) (d) relaxed sample annealed at 590K for 24h.

4. Conclusion

The effect of structural relaxation on deformation behavior of $Zr_{64.13}Cu_{15.75}Ni_{10.12}Al_{10}$ BMGs was studied by DSC and nanoindentation. The results demonstrated that thermally unstable defects can be annihilated by structure relaxation, as indicated by enthalpy recovery in the DSC curves. But this annihilation did not cause noticeable change of serrated plastic flow in the P - h curves and morphologies of indents, though hardness and elastic modulus are sensitive to this annihilation of thermally unstable defects.

Acknowledgments

We are grateful to Associate Professor H. L. Li for his help in carrying out AFM experiments. This work is financially supported by the National Nature Science Foundation of China (Grant Nos. 50571109, 10572142 and 10432050) and National Basic Research Program of China (973 Program, No. 2007CB613905).

References

1. A. L. Greer, and E. Ma, *MRS Bull.* **32**, 611 (2007).
2. J. Schroers, and W. L. Johnson, *Phys. Rev. Lett.* **93**, 4 (2004).
3. Y. H. Liu *et al.*, *Science* **315**, 1385 (2007).
4. L. Y. Chen *et al.*, *Phys. Rev. Lett.* **1**, 4 (2008).

5. D. C. Hofmann *et al.*, *Nature* **451**, 1085 (2008).
6. C. A. Schuh, T. C. Hufnagel, and U. Ramamurty, *Acta Mater.* **55**, 4067 (2007).
7. M. Q. Jiang *et al.*, *Philos. Mag.* **88**, 407 (2008).
8. M. Chen, *Ann. Rev. Mater. Res.* **38**, 445 (2008).
9. F. Spaepen, *Acta Metall.* **25**, 407 (1977).
10. F. Spaepen, in *physics of defects*, ed. R. Balian (North-Holland, 1981), p. 135.
11. A. I. Taub, and F. Spaepen, *Acta Metall.* **28**, 1781 (1980).
12. T.-W. Wu, and F. Spaepen, *Philos. Mag. B* **61**, 739 (1990).
13. U. Ramamurty *et al.*, *Scripta. Mater.* **47**, 107 (2002).
14. P. Murah, and U. Ramamurty, *Acta Mater.* **53**, 1467 (2005).
15. Y. Liu *et al.*, *Chin. Phys. Lett.* **23**, 1868 (2006).
16. N. Li *et al.*, *J. Phys. D-Appl. Phys.* **40**, 6055 (2007).
17. W. H. Jiang *et al.*, *Mater. Sci. Eng. A* **430**, 350 (2006).
18. W. H. Jiang *et al.*, *Mater. Trans.* **48**, 1781 (2007).
19. A. van den Beukel, and J. Sietsma, *Acta Metall. Mater.* **38**, 383 (1990).
20. A. Slipenyuk, and J. Eckert, *Scripta. Mater.* **50**, 39 (2004).
21. W. H. Jiang, and M. Atzmon, *J. Mater. Res.* **18**, 755 (2003).
22. C. A. Schuh, A. C. Lund, and T. G. Nieh, *Acta Mater.* **52**, 5879 (2004).
23. W. J. Wright, R. Saha, and W. D. Nix, *Mater. Trans.* **42**, 642 (2001).